The Pennsylvania State University

The Graduate School

REPRODUCIBILITY OF FUNCTIONAL CONNECTOMICS IN TRAUMATIC BRAIN INJURY

A Thesis in

Psychology

by

Hollie Mullin

Submitted in Partial Fulfillment
of the Requirements
for the Degree of

Master of Science

May 2024

The thesis of Hollie Mullin was reviewed and approved by the following:

Frank Hillary
Professor of Psychology
Thesis Advisor

Peter Arnett
Professor of Psychology

Nancy Dennis
Professor of Psychology

Kristin Buss
Professor of Psychology & Human Development and Family Studies
Head of the Department

ABSTRACT

Resting-state functional magnetic resonance imaging has the ability to provide information about brain functioning. However, it is difficult to interpret conclusions about rsfMRI data due to questions about the reliability of resting-state functional connectivity (RSFC). This study investigated the test-retest reliability of resting-state networks using a "mini" multiverse approach for individuals who have sustained traumatic brain injuries (TBIs) using back-to-back rsfMRI scans. This is an understudied area that can improve our understanding of RSFC and its potential use in clinical populations.

45 individuals with TBI and 41 healthy controls received back-to-back rsfMRI scans. 25 individuals with TBI and 15 healthy controls received another scanning session approximately 2 years after the first. The data were preprocessed with fMRIPrep. XCP_D was used to create functional connectivity matrices using 8 different brain atlases. Several graph theory metrics were calculated. Intraclass correlation coefficients (ICCs) were utilized to examine the reliability of all graph metrics for each brain atlas across each participant's back-to-back rsfMRI scans for both scanning sessions.

Results suggest that within-network connectivity, segregation, and modularity are the most reliable graph metrics, even after significant neurological compromise. The default mode network is one of the most reliable networks, whereas the limbic network is one of the least reliable networks. These results persist across the TBI and HC groups, brain atlases, and over time between the two scanning sessions, though there are some inconsistencies. This study underscores the importance of investigating the variability of ICCs. This will aid in the identification of resting-state biomarkers and will allow us to gain a better understanding of how subject characteristics and fMRI workflows impact RSFC reliability.

TABLE OF CONTENTS

LIST OF FIGURES

Figures can be found in Appendix A.

LIST OF TABLES

Tables can be found in Appendix B.

ACKNOWLEDGEMENTS

I want to thank Dr. Frank Hillary for his mentorship, guidance, and expertise throughout the development of this project. I would also like to thank Cat Carpenter for brainstorming, discussing, and assisting with this project. Additionally, I thank Dr. Pete Arnett and Dr. Nancy Dennis for serving as committee members and providing feedback. Finally, I greatly appreciate my family and friends for their endless love and support throughout my graduate school journey. I want to specifically thank my partner, Zach, for being my rock throughout this process and serving as an honorary consultant for the coding of this project.

This project is funded, in part, under a Grant from the Pennsylvania Department of Health (#4100077082). The Department specifically disclaims responsibility for any analyses, interpretations, or conclusions.

Chapter 1

Introduction

Background

The Center for Disease Control and Prevention (CDC, 2016) estimates that annually, 1.5 million Americans suffer from a traumatic brain injury (TBI). About 230,000 people are hospitalized each year from a TBI, and 2% of Americans are currently living with a disability due to a TBI (CDC, 2016). TBIs have severe impacts on cognitive abilities and daily functioning, and they typically result in widespread disruptions across brain networks (Venkatesan et al., 2015). A method of investigating these disruptions is by conducting resting-state functional connectivity (RSFC) analyses.

RSFC examines brain connections by describing statistical relationships of the blood oxygen level dependent (BOLD) signal across multiple regions while the brain is at rest and not engaged in a cognitive task (Sporns, 2013). While RSFC can be calculated in many different ways, it is commonly measured with graph theory analyses, which is a way of modeling the brain as a complex network comprised of various regions and connections (edges) between those regions (Rubinov & Sporns, 2010). Graph theory is a useful method for calculating whole-brain RSFC patterns, and brain regions can be grouped into larger brain networks to better understand brain organization and functioning (Rubinov & Sporns, 2010). At rest, certain areas of the brain are highly connected (Lee et al., 2013). For example, the default mode network (DMN) exhibits coherent neural activity at rest, but not during a task (Buckner et al., 2008). Additionally, the default, frontoparietal, and dorsal attention networks are some of the most reliable areas that demonstrate increased levels of connectivity at rest (Buckner et al., 2008; Ma et al., 2021).

Increased coherence in the DMN at rest is positively associated with semantic memory performance, and increased coherence in the frontoparietal and dorsal networks facilitate adaptive task performance and better memory abilities (Grieder et al., 2018; Franzmeier et al., 2017). Disruptions in these resting-state networks have even been linked to the onset of Alzheimer's Disease (Grieder et al., 2018). This indicates that RSFC can reveal crucial information about brain functioning and potentially serve as a biomarker for neurological disorders.

RSFC Trends for TBIs

Since TBIs are incredibly prevalent, examining RSFC post-injury is particularly important. Using a variety of graph theory metrics, studies have found that individuals who have sustained TBIs have different RSFC patterns than healthy controls. The variability of RSFC for individuals living with a TBI depends on the location and severity of the injury (Gordon et al., 2017). Venkatesan et al. (2015) found that moderate-to-severe TBI causes RSFC disruptions in the posterior cingulate cortex (PCC), anterior DMN, and hippocampal regions. The PCC is particularly susceptible to pathology and plays a central role in DMN connectivity and cognition, such as memory performance, whereas hippocampi disruptions explain impaired attentional abilities (Venkatesan et al., 2015). Bernier et al. (2017) found that individuals with moderate-to-severe TBI show hyperconnectivity within the DMN at rest. Hyperconnectivity represents a substantial increase in brain connectivity, which demonstrates an excessive increase in neural resource use, and is typical for people who have sustained a brain injury (Hillary et al., 2015). Although hyperconnectivity is thought to be an adaptive process, it may increase the risk of brain pathology, such as Alzheimer's disease, over time (Hillary & Grafman, 2017). However, it is important to note that *hypoconnectivity* can also emerge after a TBI. Contrary to hyperconnectivity, hypoconnectivity is a significant decrease in brain connectivity. For instance,

Venkatesan et al. (2015) discovered hypoconnectivity between the PCC, frontoparietal, and inferior parietal areas of the brain in addition to hyperconnectivity among other regions after moderate-to-severe TBI.

It has been observed that these alterations in RSFC after a TBI are lasting. They tend to result in long-term changes to RSFC that differ from normal brain behavior (Meier et al., 2020). Venkatesan et al. (2015) observed that RSFC adaptations in the PCC, DMN, and hippocampi regions persisted for months post-injury. Haight (2021) discovered that RSFC changes persist 3, 6, and 12 months after a TBI. Sharp et al. (2011) found that connectivity changes after TBI existed up to 6 years post-injury. Therefore, examining RSFC alterations post-injury could aid in the identification of biomarkers and guide rehabilitation interventions for patients recovering from TBIs (Lee et al., 2013).

Overview of RSFC Reliability

While RSFC has potential to be used in clinical settings, the reliability of RSFC remains unclear. Some studies have examined individual edge reliability, which is a more basic unit of brain connectivity (Noble et al., 2019). Noble et al.'s (2019) meta-analysis found that, on average, studies that examined the reproducibility of edges revealed poor reliability. In addition, Tozzi et al. (2020) found that individual brain edges range in reliability. The majority of edges had poor to fair reliability, only 6-8% of these edges had good reliability, and less than 1% of connections revealed excellent reliability (Tozzi et al., 2020). Although examining individual edge connections is a useful way of quantifying reliability, single edge reliability has been shown to be less reliable compared to graph metric reliability, which quantifies whole-brain RSFC patterns instead of individual connections (Han et al., 2024).

Rather than examining single edge reliability, recent studies have shifted their focus to evaluate the reliability of functional connectivity using graph theory measures to better quantify whole-brain RSFC patterns. Although Elliott et al. (2020) examined task functional connectivity rather than RSFC, their results are notable. Elliott et al.'s (2020) meta-analysis revealed disparate levels of functional connectivity reproducibility among brain networks during common functional magnetic resonance imaging (fMRI) tasks, ranging from poor to excellent reliability. For RSFC, Ma et al. (2021) found that while some resting-state networks had excellent reliability, most had fair to good reliability. Using a variety of different graph theory metrics, brain atlases, and preprocessing steps, Braun et al. (2012) found that average RSFC reliability was fair.

Overall, given the varying results regarding the reproducibility of functional connectivity analyses at the individual edge and whole-brain level, findings from studies that evaluate RSFC should be interpreted with caution.

Explanations for Varying Reliability

There are some explanations as to why findings from functional connectivity studies are challenging to replicate. A key issue is that there are 69,120 different workflows when preprocessing fMRI data, which can lead to disparate results (Poldrack et al., 2017). There are also many ways to analyze fMRI data once it has been preprocessed. When 70 investigators were asked to analyze the same imaging dataset with identical hypotheses, their conclusions were divergent from one another due to differing workflows (Botvinik-Nezer et al., 2020). One reason for the large number of workflows and conclusions is because the researcher defines the brain regions to examine. There are many methods that can be used to define brain regions, including a variety of brain atlases to choose from. Hallquist & Hillary (2018) determined that the average number of defined brain regions for studies falls around 1,129, but this number can range from 10

to 67,632. This makes it difficult to compare RSFC studies to one another because the locations and number of brain regions are not consistent. Furthermore, the large number of decision points, such as the use of binary or weighted connections, global signal regression, brain atlas, and graph metric choice, are known to significantly impact RSFC reliability (Andellini et al., 2015; Termenon et al., 2016).

Current Study

In summary, the lack of clarity regarding the reliability of RSFC severely limits its potential usefulness in clinical practice. Examining the test-retest reliability of RSFC for individuals who have sustained TBIs is a critical first step to not only gain a better understanding of RSFC reproducibility, but to work toward integrating neuroimaging in clinical settings.

This study investigated the reproducibility of RSFC by evaluating back-to-back resting-state fMRI (rsfMRI) scans. To our knowledge, this is the first study that evaluated the reliability of RSFC within a TBI population in comparison to healthy controls (HCs). Previous studies limited their inspections of RSFC reliability to a small set of graph theory metrics and brain atlases. As far as we know, this is the first study that utilized a wide variety of graph theory metrics to examine RSFC reliability at the whole-brain level using 8 brain atlases. In other words, the present study used an innovative “mini” multiverse approach, inspired by Dafflon et al.’s (2022) multiverse paper. This mini multiverse approach helps address the issues associated with the large number of fMRI workflows and researcher decision points that are known to affect RSFC reliability.

Aim 1

The first aim of the proposed study is to evaluate the reliability of RSFC for individuals that received back-to-back rsfMRI scans during a single fMRI scanning session (i.e., one timepoint). Overall, we predicted RSFC would be reliable. However, we predicted that canonical resting-state networks (e.g., DMN) would be more reliable than other networks. Additionally, given brain disruptions occur after TBI, we predicted that RSFC reliability may differ between HC and TBI groups, such that the TBI group may have reduced reliability. Next, we compared the reliability of RSFC using several brain atlases to determine if divergent workflows, such as atlas choice, impact reproducibility. The following research questions were examined as part of Aim 1:

1. Does RSFC remain reliable across back-to-back resting-state scans?
2. Are certain brain networks more reliable than others?
3. Does the reliability of RSFC differ between individuals with TBIs and HCs?
4. Does RSFC demonstrate more reliability when using a specific brain atlas?

Aim 2

Some subjects participated in a second fMRI scanning session that occurred about 2 years after the first scanning fMRI session. The second scanning session was also comprised of back-to-back rsfMRI scans. In addition to investigating RSFC replicability across the back-to-back scans for the second fMRI scanning session, this study examined how RSFC reliability changes over time. We compared changes in RSFC reliability between the first and second fMRI scanning sessions (i.e., two timepoints). Overall, we predicted that RSFC reliability will remain stable over time, but it may demonstrate more variability for individuals who have sustained TBIs. The following research questions were examined as part of Aim 2:

5. Across two separate fMRI scanning sessions (i.e., timepoints), does RSFC across back-to-back resting-state scans remain reliable over a ~2-year time period?
6. Are certain brain networks more reliable than others over time?
7. Are there differences in RSFC reliability between individuals with TBIs compared to HCs over time?
8. Does RSFC demonstrate more reliability when using a specific brain atlas over time?

Preregistration

Before examining the questions outlined above, we preregistered our study plan through the Open Science Framework (OSF). The preregistered design for this study is available at https://osf.io/sjaz5.

Chapter 2

Methods

Procedure

All study procedures were approved by the institutional review boards of the Pennsylvania State University and Moss Rehabilitation Research Institute. Participants signed an informed consent before participating in the current study. Participants completed a three-hour research visit. During this visit, participants completed a 60-minute fMRI scanning protocol. The protocol included structural scans, resting state scans, and task scans. For the participants with two scanning sessions, the sessions were separated by 751 (*SD* = 180) days for the TBI group and by 759 (*SD* = 99) days for HCs, on average. Participants also completed a battery of neuropsychological tests and self-report questionnaires during the study visit. These methods are reported separately (Venkatesan et al., 2020; Bernier et al., 2021; Vervoordt et al., 2021).

Participants

Participants were recruited from Pennsylvania State University, Hershey Medical Center, and the Moss Rehabilitation Research Institute. HCs were not eligible for this study if they had a history of psychiatric conditions or neurological disorders, including schizophrenia, bipolar disease, substance use disorder, or central nervous system disorders (e.g., dementia). For the TBI group, participants must have a history of complicated mild, moderate, or severe TBI at least 1 year prior to the study visit. Mild complicated TBI was classified as a GCS score of 13-15, a PTA of 0 days, but positive imaging findings of head trauma. Moderate TBI was classified as a Glascow Coma Scale (GCS) score of 9-12 and or/ Post-Traumatic Amnesia (PTA) between 1-14

days. Severe TBI was classified as a GCS score ≤ 8 and/or PTA ≥ 15 days. PTA and GCS were determined by participant self-report, interview, and/or medical records. Participant characteristics are summarized in Table 1 and Table 2.

Sample Size

The parent study is comprised of 121 participants with a history of TBI and 49 HCs (Vervoordt et al., 2021). We included only those with back-to-back rsfMRI scans in the current analysis. Based on visual inspection, 1 participant in the TBI group was removed due to excessive signal loss in their resting-state scans. For this study's final sample, the first MRI scanning session comprised of 45 (32 males) TBI participants and 41 (24 males) HCs. The second MRI scanning session comprised of 25 (16 males) TBI participants and 15 (7 males) HCs.

Imaging

Imaging data were collected on a Siemens Magnetom Trio 3T Prisma Fit scanner at Penn State Hershey Medical Center (*N*=8), an identical Siemens 3T Prisma Fit scan at Moss Rehabilitation (*N*=56), or a Siemens Prisma 3 T whole-body scanner at The Pennsylvania State University in the Social, Life, and Engineering Sciences Imaging Center at University Park (*N*=22).

Anatomical Scans

Anatomical structural scans were collected using an MPRAGEsequence at a spatial resolution of 1-mm ×1-mm ×1-mm voxels with a repetition time (TR) of 2,300 ms, echo time (TE) of 2.98 ms, and flip angle of 9°. Slices were collected interleaved.

Resting-state Scans

Participants completed two rsfMRI scans. Each scan was 10 minutes and the second rsfMRI scan took place immediately after the first rsfMRI scan. In total, two resting-state scans and 20 minutes of resting data were collected. Participants were instructed to keep their eyes open and fixate on a white cross in the center of the screen. They were also reminded to not fall asleep during the resting-state scan. The resting-state runs included 300 brain volumes with TR = 2,000 ms, TE = 30 ms, and flip angle = 90.

Preprocessing

Results included in this manuscript come from preprocessing performed using fMRIPrep 23.1.3 (Esteban et al. (2019). fMRIPrep is a standardized, preprocessing pipeline that establishes similar preprocessing steps among neuroimaging studies to enhance reproducibility.

Each subject's T1 scan, otherwise known as the T1w-reference, was referenced throughout the fMRIPrep workflow. The T1w-reference was skull-stripped with a Nipype implementation of the antsBrainExtraction.sh workflow (from ANTs), using OASIS30ANTs as target template. Brain tissue segmentation of cerebrospinal fluid (CSF), white-matter (WM) and gray-matter (GM) was performed on the brain-extracted T1w using FSL fast. Volume-based

spatial normalization to MNI space (MNI152NLin6Asym) was performed through nonlinear registration with antsRegistration using brain-extracted versions of both T1w reference and the T1w template. The transformations from T1w to MNI space were saved and later applied to transform the resting-state scans into MNI space.

For each of the back-to-back resting-state runs found per subject (across all tasks and sessions), the following preprocessing was performed. First, a reference volume and its skull-stripped version were generated using a custom methodology of fMRIPrep. Head-motion parameters with respect to the BOLD reference (transformation matrices, and six corresponding rotation and translation parameters) are estimated before any spatiotemporal filtering using FSL mcflirt. Head-motion that exceeded a threshold of 0.5 mm FD or 1.5 standardized DVARS were annotated as motion outliers. The estimated fieldmap was then aligned with rigid-registration to the target EPI (echo-planar imaging) reference run. The field coefficients were mapped on to the reference EPI using the transform. BOLD runs were slice-time corrected to 0.961s (0.5 of slice acquisition range 0s-1.92s) using 3dTshift from AFNI. Several confounding time-series were calculated based on the preprocessed BOLD: framewise displacement (FD), DVARS and three region-wise global signals (Power et al., 2014). The three global signals are extracted within the CSF, the WM, and the whole-brain masks. The BOLD time-series were resampled into standard space, generating a preprocessed BOLD run in MNI152NLin6Asym space to allow for group comparisons.

The eXtensible Connectivity Pipeline- DCAN (XCP-D) (Ciric et al. 2018; Satterthwaite et al. 2013) was used to post-process the outputs of fMRIPrep 23.1.3. For each of the four rsfMRI scans found per subject, the following post-processing steps were performed. The first four volumes of both the BOLD data and nuisance regressors were discarded as non-steady-state volumes. In total, 36 nuisance regressors were selected from the preprocessing confounds. These nuisance regressors included six motion parameters, mean global signal, mean white matter

signal, mean cerebrospinal fluid signal with their temporal derivatives, and quadratic expansion of six motion parameters, tissue signals and their temporal derivatives (Ciric et al. 2017; Satterthwaite et al. 2013). Although the regression of global signal is controversial, its removal is highly recommended given that QC metrics significantly improve (Kassinopoulos & Mitsis, 2022). It is also highly effective at minimizing motion confounds, which is relevant for our sample given that older adults are more prone to head motion in the scanner (Kassinopoulos & Mitsis, 2022; Han et al., 2024). Finally, linear trend and intercept terms were added to the regressors prior to denoising. The BOLD data were despiked with AFNI\u2019s 3dDespike, which corrects for high motion volumes without censoring entire volumes. Nuisance regressors were regressed from the BOLD data using linear regression, as implemented in Nilearn. The time series was then band-pass filtered using a(n) second-order Butterworth filter, in order to retain signals between 0.01-0.08 Hz. Spatial smoothing was not performed during preprocessing, since smoothing isn't necessary or recommended for graph theory analyses (Alakörkkö et al., 2017).

Functional Connectivity Matrices

Functional connectivity matrices, which describe the relationship between brain regions as Pearson correlation coefficients, were created for each subject (See Figure 1). Eight different matrices were created for each subject using the following atlases: the Schaefer 17-network 100, 400, 700, and 1000 parcel atlas (Schaefer et al. 2018), the Glasser atlas (Glasser et al. 2016), the Gordon atlas (Gordon et al. 2016), the Power atlas (Power et al., 2011), and the Brainnetome atlas (Fan et al., 2016). As an example, functional connectivity matrices for the Schaefer 400 atlas would result in 400 x 400 weighted connectivity matrix per subject, which describes the relationship of the 400 brain regions to one another. The diagonals in the matrices were set to NaNs since diagonals in a correlation matrix are irrelevant, given they represent the perfect

correlation between a brain region to itself. In cases of partial coverage for a given brain region, uncovered voxels (values of all zeros or NaNs) were either ignored (when the region had >50.0% coverage) or were set to NaNs (when the region had <50.0% coverage). Negative correlations were transformed to NaNs prior to graph theory analysis, given the controversy surrounding the interpretation of negative correlations (Rubinov & Sporns, 2010). Therefore, this study limited our analysis to observing only positive correlations between brain regions and didn't take negative correlations into account. This was another justification for why we performed global signal regression, since it maximizes the specificity of positive resting-state correlations (Weissenbacher et al., 2009). Lastly, the Pearson *r* correlations in all connectivity matrices were transformed to Fisher *z* values prior to analysis.

Quality Assurance

The preprocessed fMRI data were visually inspected prior to analysis to ensure data quality, based on the outputs of fMRIPrep and XCP_D. In order to account for motion in the resting-state scans, despiking in XCP_D was performed. Motion scrubbing was not performed in addition to despiking, as removing entire timepoints in fMRI data due to motion may decrease the validity and reliability of functional connectivity measurements (Phạm et al., 2023). QC metrics provided by XCP_D were evaluated to ensure artifacts and noise in the data were removed.

Data Analysis

RSFC was investigated using graph theory metrics recommended by Hallquist and Hillary (2018). These metrics were calculated by adapting scripts from the Brain Connectivity Toolbox (https://sites.google.com/site/bctnet/). The graph theory scripts for this study are publicly

available at https://github.com/holsmon/Masters/tree/main/Graph_Theory_Scripts. Graph theory metrics included within-network connectivity (strength of a region's connection to other regions within the same network), modularity (measures the degree that larger brain networks can be divided into smaller subnetworks), segregation (measures the relative strength of within-network connectivity compared to between-network connectivity), between-network connectivity (strength of a region's connection to other regions outside of the region's network), edge strength (sum of weights of links connected to a brain region), average path length (shortest-path distance between a region to all other regions), average degree (average number of regions the current region is connected to), clustering coefficient (proportion of connected regions across all neighboring regions), and eigenvector centrality (measures the influence of a particular brain region in a network). These graph metrics are explained in greater detail by Rubinov and Sporns (2010).

Test-retest reliability of RSFC were determined by intraclass correlation coefficients (ICCs), as described by Ma et al. (2021). We utilized an ICC (3,1), two-way mixed-effects model by Shrout and Fleiss (1979). This model is recommended by Koo et al. (2016) to evaluate test-retest reliability, and this model is utilized in other studies that examine functional connectivity reliability (Elliott et al., 2020; Noble et al., 2019; Ma et al., 2021). ICC values were calculated with RStudio, and the ICC code is publicly available at https://github.com/holsmon/Masters/tree/main/ICC_Code. ICCs were interpreted using the following criteria: ICCs less than 0.40 indicate poor reliability; ICCs between 0.40 and 0.60 indicate fair reliability; ICCs between 0.60 and 0.80 indicate good reliability; and ICCs greater than 0.80 indicate excellent reliability (Ma et al., 2021). An ICC was calculated for each graph theory metric to examine reliability between the back-to-back rsfMRI scans for both MRI scanning sessions.

Chapter 3

Results

Graph Metric Reliability

Within-network (WN) connectivity had good to excellent reliability on average for both scanning sessions (ICC = 0.60-0.92). There were no statistically significant differences in reliability observed in the first scanning session between the groups or atlases (see Figures 2-3). For the second scanning session, the TBI group's Schaefer 1000 atlas (ICC = 0.92, 95% CI [0.84-0.97]) had significantly better reliability compared to the TBI group's Glasser atlas (ICC = 0.65, 95% CI [0.35-0.83]). Additionally, the TBI group's Schaefer 1000 atlas from the second session had significantly better reliability than the TBI group's Gordon (ICC = 0.66, 95% CI [0.46-0.80]), Glasser (ICC = 0.68, 95% CI [0.48-0.81]), and Schaefer 400 (ICC = 0.70, 95% CI [0.51-0.82]) atlases from the first session, and the HC group's Gordon (ICC = 0.67, 95% CI [0.46-0.81]) and Glasser (ICC = 0.60, 95% CI [0.36-0.76]) atlases from the first session. These results emphasize that the Glasser and Gordon atlases have lower reliability than the other atlases (see Figures 2-3).

Modularity had fair to excellent reliability for the first scanning session on average (ICC = 0.56-0.84). The reliability of modularity declined for the second scanning session and had poor to excellent reliability on average (ICC = 0.30-85). This decline in reliability for the second session was driven by poor reliability in the Gordon atlas (ICC = 0.30-0.34). There were no significant differences between the groups or brain atlases for the first scanning session (see Figures 2-3). For the second scanning session, there was a significant difference between the TBI group's Schaefer 1000 atlas (ICC = 0.85, 95% CI [0.68-0.93]) compared to the TBI group's Power (ICC = 0.35, 95% CI [-0.04-0.65]) and Gordon (ICC = 0.34, 95% CI [-0.06-0.64]) atlases. The TBI's group's Power and Gordon atlases from the second scanning session had significantly

lower reliability compared to the TBI group's Power (ICC = 0.83, 95% CI [0.72-0.90]), Schaefer 700 (ICC = 0.81, 95% CI [0.69-0.89]), and Schaefer 1000 (ICC = 0.84, 95% CI [0.72-0.91]) atlases from the second scanning session. This indicated the Schaefer 1000 atlas was more reliable and the Gordon atlas was less reliable compared to some of the other atlases, but only for the TBI group (see Figures 2-3).

Segregation for both scanning sessions had fair to excellent reliability on average (ICC = 0.41-0.93). The segregation ICCs for the TBI group indicated better reliability than the HCs for both scanning sessions. This was more apparent in the first scanning session when comparing the TBI group (ICC = 0.65-87) to the HCs (ICC = 0.41-72), and these differences were significant for certain atlases (see Figures 2-3). For the first scanning session, the TBI group's Schaefer 100 (ICC = 0.80, 95% CI [0.66-0.88]), Power (ICC = 0.82, 95% CI [0.70-0.90]), Gordon (ICC = 0.78, 95% CI [0.64-0.87]), Schaefer 400 (ICC = 0.85, 95% CI [0.75-0.92]), Schaefer 700 (ICC = 0.87, 95% CI [0.78-0.93]), and Schaefer 1000 (ICC = 0.87, 95% CI [0.78-0.93]) atlases had significantly better reliability when compared to the HC group's Schafer 100 (ICC = 0.41, 95% CI [0.11-0.63]) and Gordon (ICC = 0.43, 95% CI [0.15-0.65]) atlases. For the second scanning session, the TBI group's Schaefer 1000 atlas (ICC = 0.92, 95% CI [0.83-0.96]) had significantly better reliability compared to the HC group's Schaefer 100 (ICC = 0.52, 95% CI [0.04-0.81]), Brainnetome (ICC = 0.41, 95% CI [-0.11-0.75]), and Gordon (ICC = 0.44, 95% CI [-0.07-0.77]) atlases, and when compared to the TBI group's Power (ICC = 0.61, 95% CI [0.29-0.81]), Gordon (ICC = 0.45, 95% CI [0.08-0.72]), and Glasser (ICC = 0.56, 95% CI [0.22-0.78]) atlases. This emphasized that the Glasser and Gordon atlases had worse reliability than some of the other atlases (see Figures 2-3). The results also suggest that when using certain brain atlases, the TBI group had significantly more reliable measures of segregation, especially for the Schaefer 1000 atlas (see Figures 2-3).

Between-network (BN) connectivity for the first and second MRI scanning session had fair to good reliability on average (ICC = 0.47-0.85). For the first scanning session, the TBI group's Power atlas (ICC = 0.85, 95% CI [0.74-0.91]) was significantly more reliable than the TBI group's Schaefer 100 (ICC = 0.50, 95% CI [0.25-0.69]) and the HC's Schaefer 100 (ICC = 0.47, 95% CI [0.19-0.68]) and Schaefer 400 (ICC = 0.65, 95% CI [0.29-0.73]) atlases. There were no significant differences between the groups or brain atlases for the second MRI scanning session. The results indicated the Power atlas had better reliability and the Schaefer 100 atlas had worse reliability than some of the other atlases (see Figures 2-3).

Edge strength for the first and second MRI scanning session had fair to good reliability on average (ICC = 0.40-0.80). There were no statistically significant differences observed within or between the two scanning sessions (see Figures 2-3). There were also no differences observed between the HC and TBI groups, and there were no differences observed between the brain atlases (see Figures 2-3).

Average path length for the first and second MRI scanning session had good to excellent reliability (ICC = 0.60-86) on average. There were no statistically significant differences observed within or between the two scanning sessions. Although this difference was not statistically significant, the average path length ICCs for the HC group (ICC = 0.64-0.86) indicated better reliability than the TBI group (ICC = 0.60-0.80) for both scanning sessions. Overall, there were no differences observed between the HC and TBI groups, and there were no differences observed between the brain atlases (see Figures 2-3).

Degree had fair to good reliability for the first scanning session on average (ICC = 0.54-0.72). For the second scanning session, degree had poor to good reliability on average (ICC = 0.37-0.79). However, there were no statistically significant differences observed within or between the two scanning sessions (see Figures 2-3). There were no differences observed

between the HC and TBI groups, and there were no differences observed between the brain atlases (see Figures 2-3).

Clustering coefficient for the first scanning session had fair to good reliability on average (ICC = 0.41-0.67). For the second scanning session, clustering coefficient had poor to good reliability on average (ICC = 0.00-0.64). However, there were no statistically significant differences observed within or between the two scanning sessions. Although this difference was not statistically significant, the clustering coefficient ICCs for the HC group (ICC = 0.58-0.67) indicated better reliability than the TBI group (ICC = 0.41-0.60), but only for the first scanning session. Overall, there were no differences observed between the HC and TBI groups, and there were no differences observed between the brain atlases (see Figures 2-3).

Eigenvector centrality for the first scanning session had poor to fair reliability on average (ICC = 0.26-0.55). For the second scanning session, eigenvector centrality had poor to good reliability on average (ICC = 0.06-0.76). There were no significant differences observed within the first scanning session, or between the first and second scanning sessions. However, for the second scanning session, the TBI group's Power atlas (ICC = 0.76, 95% CI [0.52-0.89]) had significantly higher reliability than the TBI group's Schaefer 400 atlas (ICC = 0.26, 95% CI [-0.03-0.51]) from the first scanning session. However, as a whole, there were no differences observed between the HC and TBI groups, and there were no differences observed between the brain atlases.

Brain Network Reliability

The 100 brain regions from the Schaefer100 atlas were divided into 17 networks. For both WN connectivity and segregation, ICCs were obtained for each individual network (see Figures 4-7). For the first scanning session that estimated WN connectivity, most of the ICCs fell

in the fair range (see Table 3). The TBI group's LimbicA network (ICC = 0.85, 95% CI [0.52-0.89]) had significantly greater reliability than many other networks (see Figure 4). The DorsalAttenA network for the TBI (ICC = 0.77, 95% CI [0.62-0.87]) and HC (ICC = 0.76, 95% CI [0.59-0.86]) groups had significantly better reliability than the TBI group's SomatomotorA network (ICC = 0.35, 95% CI [0.06-0.58]). For the second scanning session that estimated WN connectivity, most of the ICCs fell in the good range (see Table 3 and Figure 5). The TBI group's LimbicA network (ICC = 0.84, 95% CI [0.68-0.93]) had significantly greater reliability than the TBI group's VisualCent network (ICC = 0.08, 95% CI [-0.32-0.46]) and the HC group's ControlB network (ICC = 0.24, 95% CI [-0.29-0.66]). For the first scanning session that estimated segregation, more ICCs fell in the poor to fair range (see Table 4). The TBI group's VentralAttenB network (ICC = 0.86, 95% CI [0.75-0.92]) had significantly greater reliability than many other networks whereas the Limbic B network (ICC = 0.00, 95% CI [-0.29-0.29]) had significantly worse reliability than many other networks (see Figure 6). Additionally, the TBI group's ControlC network (ICC = 0.76, 95% CI [0.60-0.86]) had greater reliability than the HCs ControlA network (ICC = 0.24, 95% CI [-0.07-0.51]). For the second scanning session that estimated segregation, ICCs fell in the good range (see Table 4). The HC's VisualPeri network (ICC = 0.85, 95% CI [0.61-0.95]) had significantly greater reliability than many other networks (see Figure 7).

The 264 brain regions from the Power atlas were divided into 12 networks. For both WN connectivity and segregation, ICCs were obtained for each individual network (see Figures 8-11). For the first scanning session that estimated WN connectivity, ICCs fell mostly in the fair to good ranges (see Table 5). There were no significant differences between the groups or networks (see Figure 8). For the second scanning session that estimated WN connectivity, ICCs fell mostly in the good range (see Table 5). The HC group's Subcortical (ICC = 0.91, 95% CI [0.74-0.97]) and Cerebellar (ICC = 0.94, 95% CI [0.84-0.98]) networks were significantly more reliable than the

TBI group's Subcortical (ICC = 0.30, 95% CI [-0.10-0.62]) and Cerebellar (ICC = 0.50, 95% CI [0.14-0.75]) networks in addition to many other networks (see Figure 9). The Auditory network (ICC = 0.22, 95% CI [-0.19-0.56]) for the TBI group had significantly worse reliability than other networks, notably the FrontoParietal network (see Figure 9). For the first scanning session that estimated segregation, ICCs fell mostly in the fair range (see Table 5). The TBI group's Default network (ICC = 0.86, 95% CI [0.75-0.92]) had significantly greater reliability than many other networks, such as the Auditory, VentralAtten, and DorsalAtten networks (see Figure 10). For the second scanning session that estimated segregation, ICCs were more variable, and ranged from poor to excellent (see Table 5). The TBI group's FrontoParietal network (ICC = 0.85, 95% CI [0.68-0.93]) had significantly greater reliability than other networks, such as the DorsalAtten, Visual, and VentralAtten networks (see Figure 11).

The 274 brain regions from the Brainnetome atlas were divided into 17 networks. For both WN connectivity and segregation, ICCs were obtained for each individual network (see Figures 12-15). For the first scanning session that estimated WN connectivity, ICCs fell mostly in the fair range (see Table 6). The HC group's Subcortical network (ICC = 0.82, 95% CI [0.68-0.90]) had significantly greater reliability than other networks, such as the DorsalAtten and the Frontoparietal networks (see Figure 12). For the second scanning session that estimated WN connectivity, the ICCs fell mostly in the good range (see Table 6). The HC group's Subcortical (ICC = 0.88, 95% CI [0.68-0.96]) and Cerebellar (ICC = 0.89, 95% CI [0.69-0.96]) networks were greater than many other networks (see Figure 13). The TBI group's Frontopartietal1 (ICC = 0.23, 95% CI [-0.18-0.56]) network had significantly worse reliability than many other networks (see Figure 13). For the first scanning session that estimated segregation, ICCs fell mostly in the poor to fair ranges (see Table 6). The HC's Subcortical network (ICC = 0.82, 95% CI [0.69-0.94]) had significantly greater reliability than other networks, such as the DorsalAtten and FrontoParietal networks (see Figure 14). The TBI group's Frontoparietal2 network (ICC = 0.11,

95% CI [-0.18-0.39]) had significantly worse reliability than many other networks (see Figure 14). For the second scanning session that estimated segregation, ICCs varies from the poor to excellent ranges (see Table 6). The HC's Default2 (ICC = 0.87, 95% CI [0.67-0.96]) had significantly greater reliability than other networks (see Figure 15). The HC's Visual2 (ICC = 0.00, 95% CI [-0.50-0.50]), FrontoParietal3 (ICC = 0.17, 95% CI [-0.36-0.61]) and FrontoParietal4 (ICC = 0.08, 95% CI [-0.43-0.56]) networks had significantly worse reliability than many other networks (see Figure 15).

The 333 brain regions from the Gordon atlas were divided into 12 networks. For both WN connectivity and segregation, ICCs were obtained for each individual network (see Figures 16-19). For the first scanning session that estimated WN connectivity, ICCs fell in the fair to good range (see Table 7). There were no significant differences between the groups or networks (see Figure 16). For the second scanning session that estimated WN connectivity, ICCs fell mostly in the good range (see Table 7). The HC's Default network (ICC = 0.92, 95% CI [0.79-0.97]) had significantly greater reliability, especially compared to the CinguloOperc and DorsalAtten networks (see Figure 17). For the first scanning session that estimated segregation, ICCs fell mostly in the good range (see Table 7). The HC's Default network (ICC = 0.83, 95% CI [0.70-0.91]) had significantly greater reliability than many other networks, most notably the DorsalAtten network (see Figure 18). For the second scanning session that estimated segregation, ICCs varies from poor to excellent reliability (see Table 7). The HC's FrontoParietal (ICC = 0.00, 95% CI [-0.50-0.50]) and Salience (ICC = 0.06, 95% CI [-0.45-0.54]) networks had significantly lower reliability than many other networks (see Figure 19).

The 360 brain regions from the Glasser atlas were divided into 12 networks. For both WN connectivity and segregation, ICCs were obtained for each individual network (see Figures 20-23). For the first scanning session that estimated WN connectivity, ICCs fell mostly in the poor to fair ranges (see Table 8). The TBI group's Default (ICC = 0.76, 95% CI [0.60-0.86]) and

Post-multi (ICC = 0.76, 95% CI [0.58-0.85]) networks had significantly greater reliability than other networks, including the DorsalAtten, Orbito-Aff, and Auditory networks (see Figure 20). For the second scanning session that estimated WN connectivity, ICCs were more concentrated in the good range (see Table 8). However, there were no significant differences between the groups or brain atlases (see Figure 21). For the first scanning session that estimated segregation, ICCs fell mostly in the poor range (see Table 8). The TBI group's Post-Multi network (ICC = 0.68, 95% CI [0.49-0.81]) had significantly worse reliability than the HC group's Post-Multi network (ICC = 0.16, 95% CI [-0.15-0.44]) and several other networks, such as the Auditory and VentMulti networks (se Figure 22). For the second scanning session that estimated segregation, ICCs fell mostly in the poor to fair ranges (see Table 8). The TBI group's VentMulti network (ICC = 0.09, 95% CI [-0.31-0.46]) had significantly worse reliability than other networks, such as the Auditory and Somatomotor (see Figure 23).

The 400 brain regions from the Schaefer 400 atlas were divided into 17 networks. For both WN connectivity and segregation, ICCs were obtained for each individual network (see Figures 24-27). For the first scanning session that estimated WN connectivity, ICCs mostly fell in the fair to good ranges (see Table 3). The HC's DefaultB network (ICC = 0.83, 95% CI [0.70-0.90]) had significantly greater reliability than other networks, most notably the LimbicA network (see Figure 24). For the second scanning session that estimated WN connectivity, ICCs fell mostly in the good to excellent ranges (see Table 3). There were no differences observed between groups or networks (see Figure 25). For the first scanning session that estimated segregation, ICCs fell mostly in the fair to good ranges (see Table 4). The TBI group's DefaultA (ICC = 0.82, 95% CI [0.69-0.90]), VenAttnA (ICC = 0.80, 95% CI [0.66-0.88]), SomatomotorA (ICC = 0.77, 95% CI [0.62-0.87]), and TempParietal (ICC = 0.76, 95% CI [0.60-0.86]), networks had significantly greater reliability than other networks (see Figure 26). The LimbicA network for the TBI (ICC = 0.34, 95% CI [0.05-0.57]) and HC (ICC = 0.03, 95% CI [-0.28-0.33]), groups had

significantly lower reliability than many other networks (see Figure 26). For the second scanning session that estimated segregation, ICCs fell mostly in the good range (see Table 4). The DefaultA network for the TBI (ICC = 0.72, 95% CI [0.47-0.87]) and HC (ICC = 0.87, 95% CI [0.65-0.95]) group was significantly greater than many other networks (see Figure 27). The LimbicB network (ICC = 0.07, 95% CI [-0.33-0.44]) for the TBI group and the VisualPeri network (ICC = 0.00, 95% CI [-0.50-0.50]) for the HC had significantly worse reliability than other networks (see Figure 27).

The 700 brain regions from the Schaefer 700 atlas were divided into 17 networks. For both WN connectivity and segregation, ICCs were obtained for each individual network (see Figures 28-31). For the first scanning session that estimated WN connectivity, ICCs fell mostly in the good range (see Table 3). The DorsalAttenA network for the TBI (ICC = 0.78, 95% CI [0.64-0.88]) and HC (ICC = 0.73, 95% CI [0.73-0.8892]) group had significantly greater reliability than other networks (see Figure 28). The TBI group's SomatomotorA network (ICC = 0.34, 95% CI [0.05-0.57]) had significantly worse reliability than other networks (see Figure 28). For the second scanning session that estimated WN connectivity, ICCs fell mostly in the good to excellent ranges (see Table 3). The TBI group's DorsalAttenB (ICC = 0.34, 95% CI [-0.06-0.64]) and LimbicB (ICC = 0.13, 95% CI [-0.27-0.49]) had significantly worse reliability compared to other networks (see Figure 29). For the first scanning session that estimated segregation, ICCs fell mostly in the fair to good ranges (see Table 4). The TBI group's DorsalAttenA (ICC = 0.84, 95% CI [0.72-0.91]), SomatomotorB (ICC = 0.85, 95% CI [0.75-0.92]), and TempParietal (ICC = 0.79, 95% CI [0.65-0.88]) had significantly greater reliability than other networks (see Figure 30). The TBI group's DorsalAttenB network (ICC = 0.35, 95% CI [0.07-0.59]) had significantly worse reliability than other networks (see Figure 30). For the second scanning session that estimated segregation, ICCs fell mostly in the good range (see Table 4). The TBI group's VisualPeri network (ICC = 0.87, 95% CI [0.73-0.94]) had significantly greater reliability than

other networks (see Figure 31). The HC group's ControlB network (ICC = 0.00, 95% CI [-0.50-0.50]) had significantly worse reliability than other networks (see Figure 31).

The 1000 brain regions from the Schaefer 1000 atlas were divided into 17 networks. For both WN connectivity and segregation, ICCs were obtained for each individual network (see Figures 32-35). For the first scanning session that estimated WN connectivity, ICCs fell mostly in the good range (see Table 3). The DorsalAttenA network for the TBI (ICC = 0.76, 95% CI [0.60-0.86]) and HC (ICC = 0.84, 95% CI [0.72-0.91]) group had significantly greater reliability than other networks (see Figure 32). The LimbicA network, specifically for the TBI group (ICC = 0.31, 95% CI [0.03-0.55]), had significantly worse reliability than other networks (see Figure 32). For the second scanning session that estimated WN connectivity, ICCs fell mostly in the good to excellent ranges (see Table 3). The TBI group's LimbicB network (ICC = 0.08, 95% CI [-0.31-0.45]) had significantly lower reliability than the HC group's LimbicB network (ICC = 0.78, 95% CI [0.47-0.92]) and other networks (see Figure 33). For the first scanning session that estimated segregation, ICCs fell mostly in the good range (see Table 4). The TBI group's LimbicA (ICC = 0.02, 95% CI [-0.27-0.31]) and LimbicB (ICC = 0.19, 95% CI [-0.11-0.45]) networks had significantly lower reliability than other networks (see Figure 34). The TBI group's SomatomotorB network (ICC = 0.86, 95% CI [0.74-0.92]) had significantly greater reliability than other networks (see Figure 34). For the second scanning session that estimated segregation, ICCs fell more in the good to excellent ranges (see Table 4). The HC group's ControlB network (ICC = 0.00, 95% CI [-0.50-0.50]) and the TBI group's LimbicB network (ICC = 0.31, 95% CI [-0.08-0.62]) had significantly worse reliability than other networks (see Figure 35). The TBI group's DefaultA (ICC = 0.88, 95% CI [0.75-0.95]), DorsalAttenA (ICC = 0.85, 95% CI [0.70-0.93]), VenAttenA (ICC = 0.87, 95% CI [0.73-0.94]), SomatomotorA (ICC = 0.86, 95% CI [0.71-0.94]), SomatomotorB (ICC = 0.87, 95% CI [0.73-0.94]), and VisualPeri (ICC = 0.88, 95% CI [0.74-0.94]) networks had significantly greater reliability than other networks (see Figure 35).

Chapter 4

Discussion

To our knowledge, this study was the first that investigated the reliability of RSFC in a TBI population. In addition, this study utilized a mini multiverse approach to investigate RSFC reproducibility across a variety of brain atlases and graph metrics. The results suggest that RSFC can yield reproducible results, even after significant neurological compromise. Overall, the RSFC patterns suggest that RSFC reliability doesn't significantly differ between the TBI group and HCs, but there were some discrepancies.

Interestingly, segregation for the TBI group had significantly better reliability than the HC group for many of the brain atlases, especially in the first scanning session. Some studies have observed that enhanced connectivity emerges within networks post-injury (e.g., hyperconnectivity) rather than between networks, which can yield increased measures of segregation (Bernier et al., 2017). This may explain why segregation reliability for the TBI group was significantly better than the HCs for certain atlases, given that prior work has found that stronger connections increase reliability (Noble et al., 2019). However, this justification doesn't explain why WN connectivity didn't differ between the TBI and HC groups a majority of the time. Contrary to Noble et al. (2019), other studies observed that stronger connections don't necessarily increase RSFC reliability (Ma et al., 2021; Tozzi et al., 2020). Additionally, significant differences in segregation reliability between the TBI and HC groups weren't prevalent for the second scanning session, though this may be due to a smaller sample size. As a whole, it is still unclear why segregation reliability may increase post-injury, and this question warrants further research.

Our study also provides novel information about the reliability patterns for a wide variety of graph metrics. WN connectivity, modularity, segregation, and average path length

demonstrated good reliability as a whole. BN connectivity, strength, and degree fell in the fair range. Clustering coefficient and eigenvector centrality had worse reliability when compared to the other metrics. Eigenvector centrality had the worst reliability overall, with ICC averages in the poor range for nearly every brain atlas. These reliability patterns were similar across the TBI and HC groups and remained similar between the first and second scanning sessions. Similar to our results, Braun et al. (2012) found that modularity had increased reliability compared to the clustering coefficient. Termenon et al. (2016) also found that the clustering coefficient was a worse measure of reliability.

Our study supported the assertation that graph metrics are more reliable than individual edge connections, given that edge connections typically result in poor reliability overall (Noble et al., 2019; Tozzi et al., 2020). Additionally, our study suggests that network-level graph metrics (e.g., WN connectivity, segregation, modularity) yield greater reliability than other metrics. This may be because other metrics are influenced more by inconsistent, edge-level connections at the whole-brain level. However, despite these overall patterns, it was difficult to compare our graph metric results to other studies. Most studies haven't evaluated reliability for a wide range of graph metrics, which makes it challenging to generalize these conclusions.

When the brain regions in the atlases were broken down into networks, it became incredibly difficult to find networks that were consistently more reliable than others. However, there were a few networks that demonstrated good to excellent reliability. For nearly all the brain atlases, at least one of the default mode networks was the most reliable for the TBI and HC groups. This pattern remained consistent over time. Matching our results, other studies have continuously reported that the DMN is one of the most reproducible networks (Elliott et al., 2019; Ma et al., 2021; Laumann et al., 2015; Noble et al., 2019). Although the limbic networks were reliable in some cases, this varied greatly. Limbic network reliability was inconsistent with ICCs ranging from poor to excellent, and this trend remained stable over time. Other studies have

reported inconsistent levels of reproducibility for the limbic networks as well (Elliott et al., 2019; Noble et al., 2019). We also found that the dorsal attention networks were as inconsistent as the limbic networks. This result was surprising, given that Ma et al. (2021) found the dorsal networks to be reliable.

Given the variety of results, we found it challenging to obtain generalizable results regarding brain network reliability. While many networks performed well for a certain atlas, they did not perform as well for another. For instance, although the frontoparietal network performed well in the Power atlas, it performed worse in the Brainnetome and Gordon atlases. While this pattern matches results from Elliott et al. (2019), which found good reliability for the frontoparietal network using the Power atlas, it is unclear why frontoparietal network reliability decreased in the other atlases. This suggests that it may be difficult to compare network-level results across different atlases, even if the atlases have the same network labels. This was also true of certain networks across time. While the somatomotor network had poor to fair reliability at the first scanning session, it had good to excellent reliability at the second scanning session for the Schaefer atlases. Inconsistency in somatomotor network reliability also exists when comparing previous studies, given that Ma et al. (2021) observed low reliability and Laumann et al. (2015) observed high reliability in this network. Another interesting discovery we observed was that the HC's subcortical and cerebellar networks were significantly more reliable than the TBI group. This was inconsistent with Noble et al.'s (2019) finding that the subcortical network was one of the least reliable networks. As for the cerebellar network, Noble et al. (2019) found that the cerebellar network ranged from poor to excellent reliability.

A possible reason for the discrepancies between brain network reliability may be due to divergent parcellation schemes. For instance, for each network, a given atlas has a differing number of regions that make up that network. Although our study didn't yield significant differences in atlas performance based on the whole-brain atlas size, it is possible that there may

be differences at the network-level. Another reason for the discrepancies in brain network reliability may depend on the atlas being used. For instance, the Glasser atlas performed consistently worse than the other atlases. Notably, the Glasser atlas was originally created using data from 210 young, healthy adults between the ages of 22-35 (Glasser et al., 2016). In addition, the Glasser atlas was constructed based on cortical architecture, which has been known to change substantially over the lifespan (Sanders et al., 2022). Therefore, it is possible that the Glasser atlas had a worse match to our specific sample, given that our dataset was comprised of older adults. This emphasizes the importance of atlas choice, and further research is needed to investigate how the creation of atlases may affect RSFC reproducibility.

Another point of consideration when evaluating network reliability is the underlying function of a given network. The DMN is highly linked to memory retrieval and envisioning the future, and a participant is likely to engage in these types of tasks during a resting-state scan (Buckner et al., 2008). Therefore, the DMN may be more representative of RSFC compared to other networks. Our results suggest the DMN could serve as a starting point for integrating RSFC into clinical settings, given that it seems to be a reliable biomarker that is conducive to rsfMRI.

Lastly, our results revealed that a lower sample size for the second scanning session impacted ICC values. Reliability was much more variable for the second sessions, as indicated by larger confidence intervals. While this makes logical sense, this underscores the importance of how small sample sizes impact reliability results, especially in the field of neuroimaging.

Limitations

A limitation for our particular study is that our sample is comprised of older adults. Additionally, our TBI participants were several years post-injury, on average. Trends in reliability may be substantially affected when examining RSFC in an individual who more recently

sustained a TBI. Future studies should explore how participant characteristics, such as age and time post-injury, may impact reproducibility. Additionally, the present study didn't evaluate how graph metric characteristics, such as weakness or strength of a given metric, affect RSFC reproducibility. We also didn't evaluate how the number of regions in a given network may affect reliability. Further investigations are needed to explore how graph metric characteristics and network properties affect RSFC reliability. In addition, our second scanning session had a smaller sample size than our first, which results in larger confidence intervals around the mean ICCs. It's imperative that future work continues to conduct longitudinal research with larger sample sizes, so that results are more generalizable.

Another factor worth considering is resting-state scan length, which has considerable effects on RSFC reliability (Han et al., 2024). Scans that are less than 5 minutes long significantly worse reliability than scans over 5 minutes (Birn et al., 2013; Braun et al., 2012). In addition, scans less than 10 minutes long have detrimental effects on graph metric reliability (Han et al., 2024). Future work can integrate longer resting-state scans into MRI protocols, which will allow the field to work towards reliable, RSFC biomarkers.

Conclusion

Overall, these results provide instrumental insight about RSFC reliability using a mini multiverse approach. To our knowledge, this study is the first to examine RSFC reliability for individuals who have sustained TBIs. Our results suggest RSFC yields reproducible results, even after significant neurological compromise. However, it is critical to continue examining factors that may impact RSFC reproducibility and its validity. We must work toward a better understanding of the factors that may impact RSFC reliability and how we can best utilize information from RSFC in clinical settings.

References

Alakörkkö, T., Saarimäki, H., Glerean, E., Saramäki, J., & Korhonen, O. (2017). Effects of spatial smoothing on functional brain networks. The European journal of neuroscience, 46(9), 2471–2480. https://doi.org/10.1111/ejn.13717

Andellini, M., Cannatà, V., Gazzellini, S., Bernardi, B., & Napolitano, A. (2015). Test-retest reliability of graph metrics of resting state MRI functional brain networks: A review. Journal of neuroscience methods, 253, 183–192. https://doi.org/10.1016/j.jneumeth.2015.05.020

Bernier, R. A., Roy, A., Venkatesan, U. M., Grossner, E. C., Brenner, E. K., & Hillary, F. G. (2017). Dedifferentiation Does Not Account for Hyperconnectivity after Traumatic Brain Injury. *Frontiers in neurology*, *8*, 297. https://doi.org/10.3389/fneur.2017.00297

Bernier, R. A., Venkatesan, U. M., Soto, J. A., Rabinowitz, A. R., Hong, J. S., & Hillary, F. G. (2021). Perceived discrimination and blood pressure in individuals aging with traumatic brain injury. Rehabilitation psychology, 66(2), 148–159. https://doi.org/10.1037/rep0000379

Birn, R. M., Molloy, E. K., Patriat, R., Parker, T., Meier, T. B., Kirk, G. R., Nair, V. A., Meyerand, M. E., & Prabhakaran, V. (2013). The effect of scan length on the reliability of resting-state fMRI connectivity estimates. NeuroImage, 83, 550–558. https://doi.org/10.1016/j.neuroimage.2013.05.099

Botvinik-Nezer, R., Holzmeister, F., Camerer, C. F., Dreber, A., Huber, J., Johannesson, M., Kirchler, M., Iwanir, R., Mumford, J. A., Adcock, R. A., Avesani, P., Baczkowski, B. M., Bajracharya, A., Bakst, L., Ball, S., Barilari, M., Bault, N., Beaton, D., Beitner, J., Benoit, R. G., … Schonberg, T. (2020). Variability in the analysis of a single

neuroimaging dataset by many teams. Nature, 582(7810), 84–88. https://doi.org/10.1038/s41586-020-2314-9

Braun, U., Plichta, M. M., Esslinger, C., Sauer, C., Haddad, L., Grimm, O., Mier, D., Mohnke, S., Heinz, A., Erk, S., Walter, H., Seiferth, N., Kirsch, P., & Meyer-Lindenberg, A. (2012). Test-retest reliability of resting-state connectivity network characteristics using fMRI and graph theoretical measures. NeuroImage, 59(2), 1404–1412. https://doi.org/10.1016/j.neuroimage.2011.08.044

Buckner, R. L., Andrews-Hanna, J. R., & Schacter, D. L. (2008). The brain's default network: anatomy, function, and relevance to disease. *Annals of the New York Academy of Sciences*, *1124*, 1–38. https://doi.org/10.1196/annals.1440.011

Centers for Disease Control and Prevention. (2016). *Report to Congress: Traumatic Brain Injury in the United States.* https://www.cdc.gov/traumaticbraininjury/pubs/tbi_report_to_congress.html#

Dafflon, J., F Da Costa, P., Váša, F., Monti, R. P., Bzdok, D., Hellyer, P. J., Turkheimer, F., Smallwood, J., Jones, E., & Leech, R. (2022). A guided multiverse study of neuroimaging analyses. Nature communications, 13(1), 3758. https://doi.org/10.1038/s41467-022-31347-8

Elliott, M. L., Knodt, A. R., Cooke, M., Kim, M. J., Melzer, T. R., Keenan, R., Ireland, D., Ramrakha, S., Poulton, R., Caspi, A., Moffitt, T. E., & Hariri, A. R. (2019). General functional connectivity: Shared features of resting-state and task fMRI drive reliable and heritable individual differences in functional brain networks. NeuroImage, 189, 516–532. https://doi.org/10.1016/j.neuroimage.2019.01.068

Elliott, M. L., Knodt, A. R., Ireland, D., Morris, M. L., Poulton, R., Ramrakha, S., Sison, M. L., Moffitt, T. E., Caspi, A., & Hariri, A. R. (2020). What Is the Test-Retest Reliability of Common Task-Functional MRI Measures? New Empirical Evidence and a Meta-

Analysis. *Psychological Science, 31*(7), 792–806. https://doi.org/10.1177/0956797620916786

Esteban, O., Markiewicz, C. J., Blair, R. W., Moodie, C. A., Isik, A. I., Erramuzpe, A., Kent, J. D., Goncalves, M., DuPre, E., Snyder, M., Oya, H., Ghosh, S. S., Wright, J., Durnez, J., Poldrack, R. A., & Gorgolewski, K. J. (2019). fMRIPrep: a robust preprocessing pipeline for functional MRI. Nature methods, 16(1), 111–116. https://doi.org/10.1038/s41592-018-0235-4

Fan, L., Li, H., Zhuo, J., Zhang, Y., Wang, J., Chen, L., Yang, Z., Chu, C., Xie, S., Laird, A. R., Fox, P. T., Eickhoff, S. B., Yu, C., & Jiang, T. (2016). The Human Brainnetome Atlas: A New Brain Atlas Based on Connectional Architecture. Cerebral cortex (New York, N.Y. : 1991), 26(8), 3508–3526. https://doi.org/10.1093/cercor/bhw157

Franzmeier, N., Göttler, J., Grimmer, T., Drzezga, A., Áraque-Caballero, M. A., Simon-Vermot, L., Taylor, A. N. W., Bürger, K., Catak, C., Janowitz, D., Müller, C., Duering, M., Sorg, C., & Ewers, M. (2017). Resting-State Connectivity of the Left Frontal Cortex to the Default Mode and Dorsal Attention Network Supports Reserve in Mild Cognitive Impairment. Frontiers in aging neuroscience, 9, 264. https://doi.org/10.3389/fnagi.2017.00264

Glasser, M. F., Coalson, T. S., Robinson, E. C., Hacker, C. D., Harwell, J., Yacoub, E., Ugurbil, K., Andersson, J., Beckmann, C. F., Jenkinson, M., Smith, S. M., & Van Essen, D. C. (2016). A multi-modal parcellation of human cerebral cortex. Nature, 536(7615), 171–178. https://doi.org/10.1038/nature18933

Gordon, E. M., Laumann, T. O., Adeyemo, B., & Petersen, S. E. (2017). Individual Variability of the System-Level Organization of the Human Brain. Cerebral cortex (New York, N.Y. : 1991), 27(1), 386–399. https://doi.org/10.1093/cercor/bhv239

Gordon, E. M., Laumann, T. O., Adeyemo, B., Huckins, J. F., Kelley, W. M., & Petersen, S. E. (2016). Generation and Evaluation of a Cortical Area Parcellation from Resting-State Correlations. Cerebral cortex (New York, N.Y. : 1991), 26(1), 288–303. https://doi.org/10.1093/cercor/bhu239

Grieder, M., Wang, D. J. J., Dierks, T., Wahlund, L. O., & Jann, K. (2018). Default Mode Network Complexity and Cognitive Decline in Mild Alzheimer's Disease. Frontiers in neuroscience, 12, 770. https://doi.org/10.3389/fnins.2018.00770

Haight, Emily J., "Functional Connectivity Changes in the Default Mode Network in Moderate-to-Severe Traumatic Brain Injury" (2021). *CUNY Academic Works.* https://academicworks.cuny.edu/gc_etds/4360

Hallquist, M. N., & Hillary, F. G. (2018). Graph theory approaches to functional network organization in brain disorders: A critique for a brave new small-world. *Network neuroscience (Cambridge, Mass.)*, *3*(1), 1–26. https://doi.org/10.1162/netn_a_00054

Han, L., Chan, M. Y., Agres, P. F., Winter-Nelson, E., Zhang, Z., & Wig, G. S. (2024). Measures of resting-state brain network segregation and integration vary in relation to data quantity: implications for within and between subject comparisons of functional brain network organization. Cerebral cortex (New York, N.Y. : 1991), 34(2), bhad506. https://doi.org/10.1093/cercor/bhad506

Hillary, F. G., & Grafman, J. H. (2017). Injured Brains and Adaptive Networks: The Benefits and Costs of Hyperconnectivity. *Trends in cognitive sciences*, *21*(5), 385–401. https://doi.org/10.1016/j.tics.2017.03.003

Hillary, F. G., Roman, C. A., Venkatesan, U., Rajtmajer, S. M., Bajo, R., & Castellanos, N. D. (2015). Hyperconnectivity is a fundamental response to neurological disruption. *Neuropsychology*, *29*(1), 59–75. https://doi.org/10.1037/neu0000110

Kassinopoulos, M., & Mitsis, G. D. (2022). A multi-measure approach for assessing the performance of fMRI preprocessing strategies in resting-state functional connectivity. Magnetic resonance imaging, 85, 228–250. https://doi.org/10.1016/j.mri.2021.10.028

Laumann, T. O., Gordon, E. M., Adeyemo, B., Snyder, A. Z., Joo, S. J., Chen, M. Y., Gilmore, A. W., McDermott, K. B., Nelson, S. M., Dosenbach, N. U., Schlaggar, B. L., Mumford, J. A., Poldrack, R. A., & Petersen, S. E. (2015). Functional System and Areal Organization of a Highly Sampled Individual Human Brain. Neuron, 87(3), 657–670. https://doi.org/10.1016/j.neuron.2015.06.037

Lee, M. H., Smyser, C. D., & Shimony, J. S. (2013). Resting-state fMRI: a review of methods and clinical applications. *AJNR. American journal of neuroradiology*, *34*(10), 1866–1872. https://doi.org/10.3174/ajnr.A3263

Ma, Y., & MacDonald Iii, A. W. (2021). Impact of Independent Component Analysis Dimensionality on the Test-Retest Reliability of Resting-State Functional Connectivity. *Brain connectivity, 11(10),* 875–886. https://doi.org/10.1089/brain.2020.0970

Meier, T. B., Giraldo-Chica, M., España, L. Y., Mayer, A. R., Harezlak, J., Nencka, A. S., Wang, Y., Koch, K. M., Wu, Y. C., Saykin, A. J., Giza, C. C., Goldman, J., DiFiori, J. P., Guskiewicz, K. M., Mihalik, J. P., Brooks, A., Broglio, S. P., McAllister, T., & McCrea, M. A. (2020). Resting-State fMRI Metrics in Acute Sport-Related Concussion and Their Association with Clinical Recovery: A Study from the NCAA-DOD CARE Consortium. *Journal of neurotrauma*, *37*(1), 152–162. https://doi.org/10.1089/neu.2019.6471

Noble, S., Scheinost, D., & Constable, R. T. (2019). A decade of test-retest reliability of functional connectivity: A systematic review and meta-analysis. *NeuroImage*, *203*, 116157. https://doi.org/10.1016/j.neuroimage.2019.116157

Phạm, D. Đ., McDonald, D. J., Ding, L., Nebel, M. B., & Mejia, A. F. (2023). Less is more: balancing noise reduction and data retention in fMRI with data-driven scrubbing. NeuroImage, 270, 119972. https://doi.org/10.1016/j.neuroimage.2023.119972

Power, J. D., Cohen, A. L., Nelson, S. M., Wig, G. S., Barnes, K. A., Church, J. A., Vogel, A. C., Laumann, T. O., Miezin, F. M., Schlaggar, B. L., & Petersen, S. E. (2011). Functional network organization of the human brain. Neuron, 72(4), 665–678. https://doi.org/10.1016/j.neuron.2011.09.006

Poldrack, R. A., Baker, C. I., Durnez, J., Gorgolewski, K. J., Matthews, P. M., Munafò, M. R., ... & Yarkoni, T. (2017). Scanning the horizon: towards transparent and reproducible neuroimaging research. *Nature reviews neuroscience*, *18*(2), 115-126. https://doi.org/10.1038/nrn.2016.167

Priestley, D., Staph, J., Koneru, S., Rajtmajer, S., & Hillary, F. (2022). Establishing ground truth in the clinical neurosciences: if replication is the answer, then what are the questions?.

Rubinov, M., & Sporns, O. (2010). Complex network measures of brain connectivity: uses and interpretations. NeuroImage, 52(3), 1059–1069. https://doi.org/10.1016/j.neuroimage.2009.10.003

Sanders, A. F. P., Baum, G. L., Harms, M. P., Kandala, S., Bookheimer, S. Y., Dapretto, M., Somerville, L. H., Thomas, K. M., Van Essen, D. C., Yacoub, E., & Barch, D. M. (2022). Developmental trajectories of cortical thickness by functional brain network: The roles of pubertal timing and socioeconomic status. Developmental cognitive neuroscience, 57, 101145. https://doi.org/10.1016/j.dcn.2022.101145

Schaefer, A., Kong, R., Gordon, E. M., Laumann, T. O., Zuo, X. N., Holmes, A. J., Eickhoff, S. B., & Yeo, B. T. T. (2018). Local-Global Parcellation of the Human Cerebral Cortex from Intrinsic Functional Connectivity MRI. Cerebral cortex (New York, N.Y. : 1991), 28(9), 3095–3114. https://doi.org/10.1093/cercor/bhx179

Sharp, D. J., Beckmann, C. F., Greenwood, R., Kinnunen, K. M., Bonnelle, V., De Boissezon, X., Powell, J. H., Counsell, S. J., Patel, M. C., & Leech, R. (2011). Default mode network functional and structural connectivity after traumatic brain injury. Brain : a journal of neurology, 134(Pt 8), 2233–2247. https://doi.org/10.1093/brain/awr175

Shrout P. E., Fleiss J. L. (1979). Intraclass correlations: Uses in assessing rater reliability. Psychological Bulletin, 86, 420–428.

Sporns O. (2013). Structure and function of complex brain networks. *Dialogues in clinical neuroscience*, *15*(3), 247–262. https://doi.org/10.31887/DCNS.2013.15.3/osporns

Tenovuo, O., Diaz-Arrastia, R., Goldstein, L. E., Sharp, D. J., van der Naalt, J., & Zasler, N. D. (2021). Assessing the Severity of Traumatic Brain Injury-Time for a Change?. *Journal of clinical medicine*, *10*(1), 148. https://doi.org/10.3390/jcm10010148

Termenon, M., Jaillard, A., Delon-Martin, C., & Achard, S. (2016). Reliability of graph analysis of resting state fMRI using test-retest dataset from the Human Connectome Project. NeuroImage, 142, 172–187. https://doi.org/10.1016/j.neuroimage.2016.05.062

Tozzi, S. L., Fleming, S. L., Taylor, Z. D., Raterink, C. D., & Williams, L. M. (2020). Test-retest reliability of the human functional connectome over consecutive days: identifying highly reliable portions and assessing the impact of methodological choices. Network neuroscience (Cambridge, Mass.), 4(3), 925–945. https://doi.org/10.1162/netn_a_00148

Venkatesan, U. M., Dennis, N. A., & Hillary, F. G. (2015). Chronology and chronicity of altered resting-state functional connectivity after traumatic brain injury. *Journal of neurotrauma*, *32*(4), 252–264. https://doi.org/10.1089/neu.2013.3318

Venkatesan, U. M., Rabinowitz, A. R., & Riccitello, R. M. (2021). Breaking the Percent Memory Retention Ceiling using Bayesian Statistics. Journal of the International Neuropsychological Society : JINS, 27(4), 396–400. https://doi.org/10.1017/S1355617720000892

Vervoordt, S. M., Arnett, P., Engeland, C., Rabinowitz, A. R., & Hillary, F. G. (2021). Depression associated with APOE status and hippocampal volume but not cognitive decline in older adults aging with traumatic brain injury. Neuropsychology, 35(8), 863–875. https://doi.org/10.1037/neu0000750

Weissenbacher, A., Kasess, C., Gerstl, F., Lanzenberger, R., Moser, E., & Windischberger, C. (2009). Correlations and anticorrelations in resting-state functional connectivity MRI: a quantitative comparison of preprocessing strategies. NeuroImage, 47(4), 1408–1416. https://doi.org/10.1016/j.neuroimage.2009.05.005

Appendix A

Figures

Figure 1
Resting-state Preprocessing

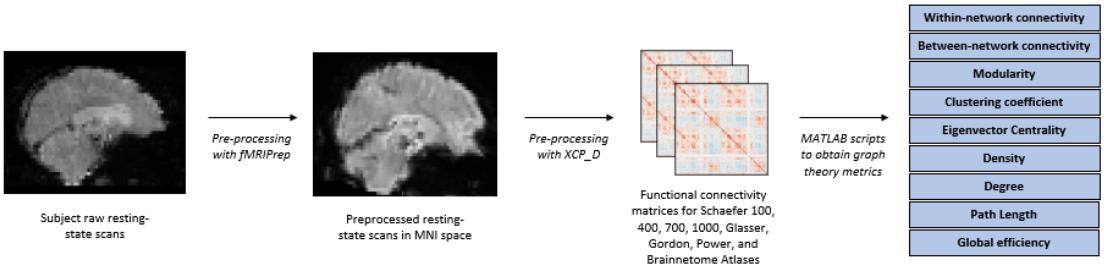

Figure 2

ICCs Session 1: All Graph Metrics

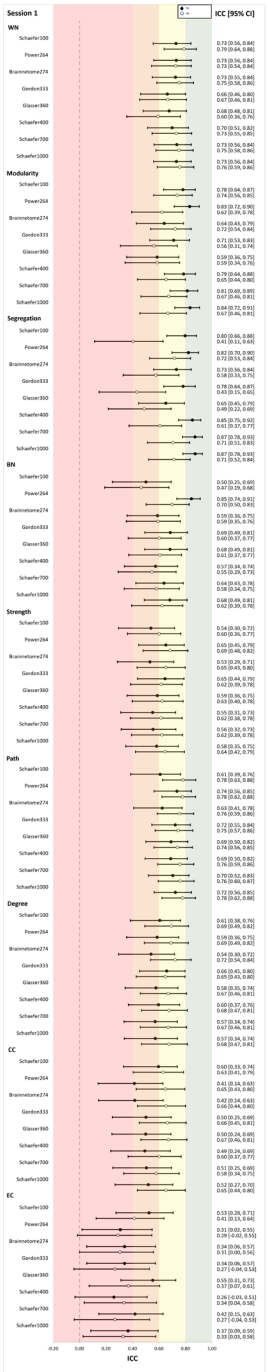

Note. Values are ICCs along with 95% confidence interval in brackets. ICCs are provided for each graph metric and brain atlas. WN = within-network connectivity; BN = between-network connectivity; Strength = average global edge strength; Path = average shortest path length; CC = clustering coefficient; EC= eigenvector centrality.

Figure 3

ICCs Session 2: All Graph Metrics

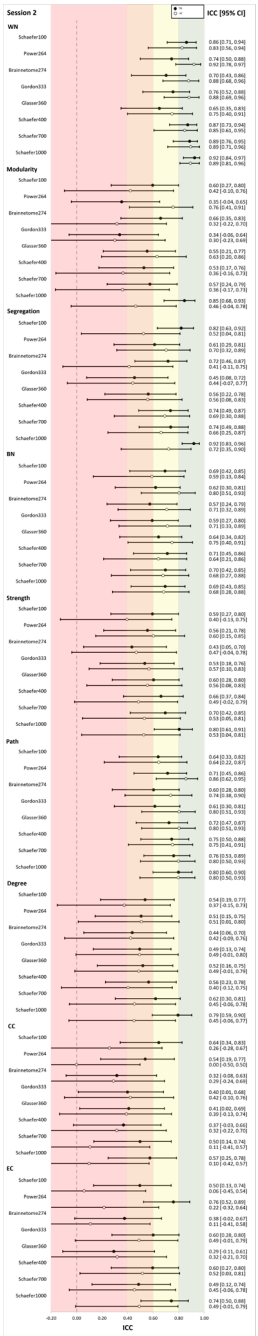

Note. Values are ICCs along with 95% confidence interval in brackets. ICCs are provided for each graph metric and brain atlas. WN = within-network connectivity; BN = between-network connectivity; Strength = average global edge strength; Path = average shortest path length; CC = clustering coefficient; EC= eigenvector centrality.

Figure 4

ICCs Session 1: Schaefer 100 WN Reliability

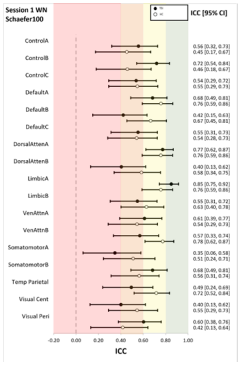

Note. Values are ICCs along with 95% confidence interval in brackets. ICCs are provided for each of the 17 networks in the Schaefer 100 atlas. WN = within-network connectivity.

Figure 5

ICCs Session 2: Schaefer 100 WN Reliability

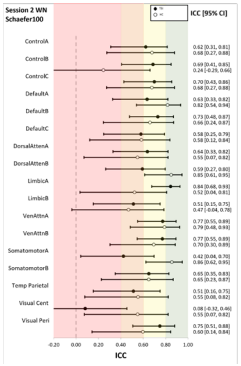

Note. Values are ICCs along with 95% confidence interval in brackets. ICCs are provided for each of the 17 networks in the Schaefer 100 atlas. WN = within-network connectivity.

Figure 6

ICCs Session 1: Schaefer 100 Segregation Reliability

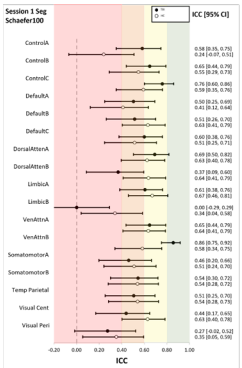

Note. Values are ICCs along with 95% confidence interval in brackets. ICCs are provided for each of the 17 networks in the Schaefer 100 atlas. Seg = segregation.

Figure 7

ICCs Session 2: Schaefer 100 Segregation Reliability

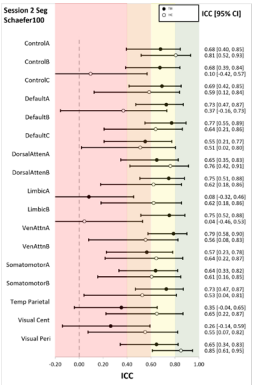

Note. Values are ICCs along with 95% confidence interval in brackets. ICCs are provided for each of the 17 networks in the Schaefer 100 atlas. Seg = segregation.

Figure 8

ICCs Session 1: Power WN Reliability

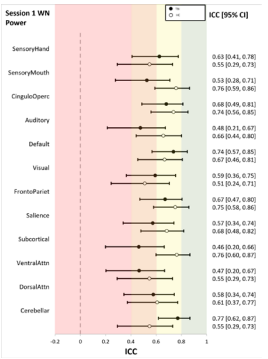

Note. Values are ICCs along with 95% confidence interval in brackets. ICCs are provided for each of the 17 networks in the Power atlas. WN = within-network connectivity.

Figure 9

ICCs Session 2: Power WN Reliability

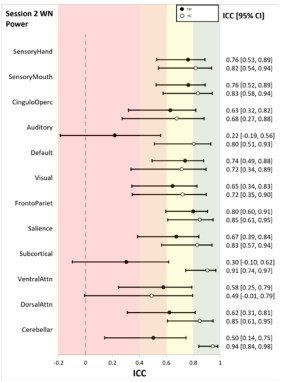

Note. Values are ICCs along with 95% confidence interval in brackets. ICCs are provided for each of the 17 networks in the Power atlas. WN = within-network connectivity.

Figure 10

ICCs Session 1: Power Segregation Reliability

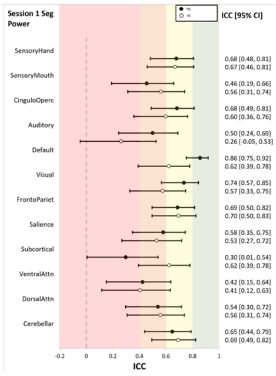

Note. Values are ICCs along with 95% confidence interval in brackets. ICCs are provided for each of the 17 networks in the Power atlas. Seg = segregation.

Figure 11

ICCs Session 2: Power Segregation Reliability

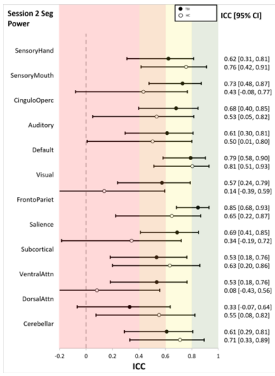

Note. Values are ICCs along with 95% confidence interval in brackets. ICCs are provided for each of the 17 networks in the Power atlas. Seg = segregation.

Figure 12

ICCs Session 1: Brainnetome WN Reliability

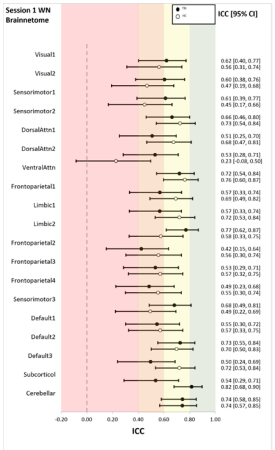

Note. Values are ICCs along with 95% confidence interval in brackets. ICCs are provided for each of the 17 networks in the Brainnetome atlas. WN = within-network connectivity.

Figure 13

ICCs Session 2: Brainnetome WN Reliability

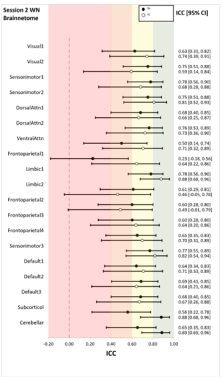

Note. Values are ICCs along with 95% confidence interval in brackets. ICCs are provided for each of the 17 networks in the Brainnetome atlas. WN = within-network connectivity.

Figure 14

ICCs Session 1: Brainnetome Segregation Reliability

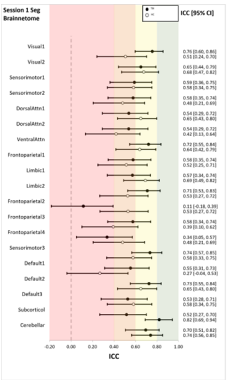

Note. Values are ICCs along with 95% confidence interval in brackets. ICCs are provided for each of the 17 networks in the Brainnetome atlas. Seg = segregation.

Figure 15

ICCs Session 2: Brainnetome Segregation Reliability

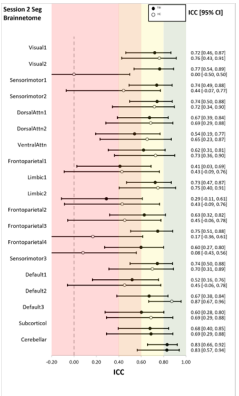

Note. Values are ICCs along with 95% confidence interval in brackets. ICCs are provided for each of the 17 networks in the Brainnetome atlas. Seg = segregation.

Figure 16

ICCs Session 1: Gordon WN Reliability

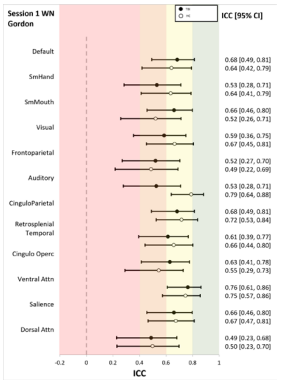

Note. Values are ICCs along with 95% confidence interval in brackets. ICCs are provided for each of the 17 networks in the Gordon atlas. WN = within-network connectivity.

Figure 17

ICCs Session 2: Gordon WN Reliability

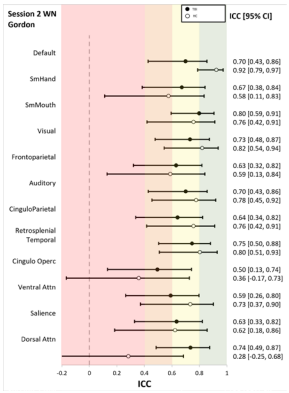

Note. Values are ICCs along with 95% confidence interval in brackets. ICCs are provided for each of the 17 networks in the Gordon atlas. WN = within-network connectivity.

Figure 18

ICCs Session 1: Gordon Segregation Reliability

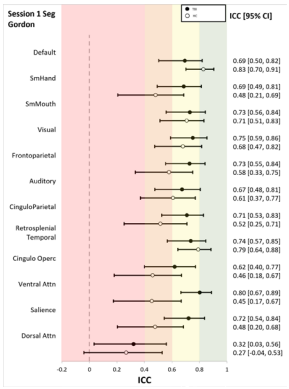

Note. Values are ICCs along with 95% confidence interval in brackets. ICCs are provided for each of the 17 networks in the Gordon atlas. Seg = segregation.

Figure 19

ICCs Session 2: Gordon Segregation Reliability

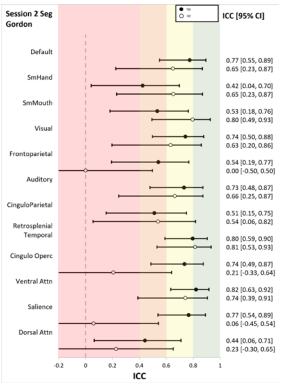

Note. Values are ICCs along with 95% confidence interval in brackets. ICCs are provided for each of the 17 networks in the Gordon atlas. Seg = segregation.

Figure 20

ICCs Session 1: Glasser WN Reliability

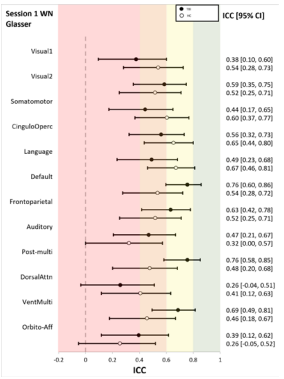

Note. Values are ICCs along with 95% confidence interval in brackets. ICCs are provided for each of the 17 networks in the Glasser atlas. WN = within-network connectivity.

Figure 21

ICCs Session 2: Glasser WN Reliability

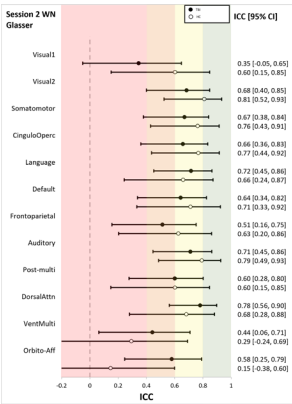

Note. Values are ICCs along with 95% confidence interval in brackets. ICCs are provided for each of the 17 networks in the Glasser atlas. WN = within-network connectivity.

Figure 22

ICCs Session 1: Glasser Segregation Reliability

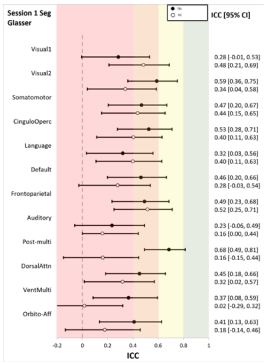

Note. Values are ICCs along with 95% confidence interval in brackets. ICCs are provided for each of the 17 networks in the Glasser atlas. Seg = segregation.

Figure 23

ICCs Session 2: Glasser Segregation Reliability

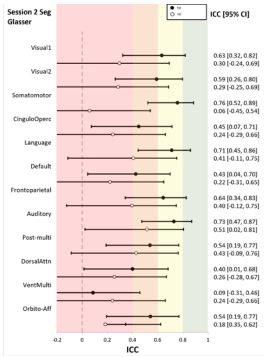

Note. Values are ICCs along with 95% confidence interval in brackets. ICCs are provided for each of the 17 networks in the Glasser atlas. Seg = segregation.

Figure 24

ICCs Session 1: Schaefer 400 WN Reliability

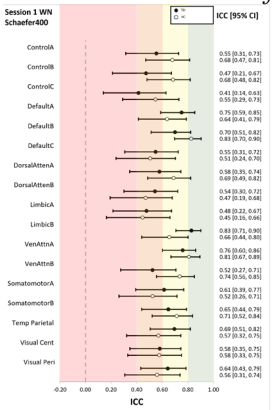

Note. Values are ICCs along with 95% confidence interval in brackets. ICCs are provided for each of the 17 networks in the Schaefer 400 atlas. WN = within-network connectivity.

Figure 25

ICCs Session 2: Schaefer 400 WN Reliability

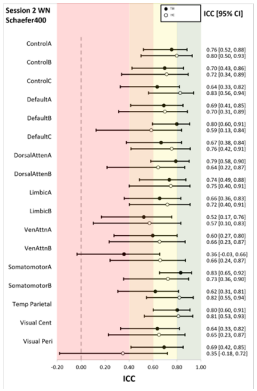

Note. Values are ICCs along with 95% confidence interval in brackets. ICCs are provided for each of the 17 networks in the Schaefer 400 atlas. WN = within-network connectivity.

Figure 26

ICCs Session 1: Schaefer 400 Segregation Reliability

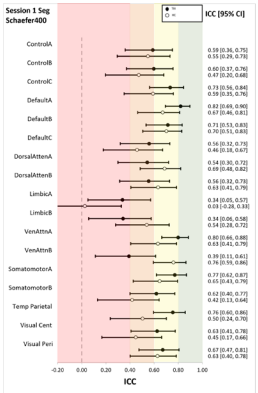

Note. Values are ICCs along with 95% confidence interval in brackets. ICCs are provided for each of the 17 networks in the Schaefer 400 atlas. Seg = segregation.

Figure 27

ICCs Session 2: Schaefer 400 Segregation Reliability

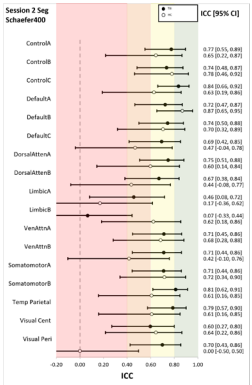

Note. Values are ICCs along with 95% confidence interval in brackets. ICCs are provided for each of the 17 networks in the Schaefer 400 atlas. Seg = segregation.

Figure 28

ICCs Session 1: Schaefer 700 WN Reliability

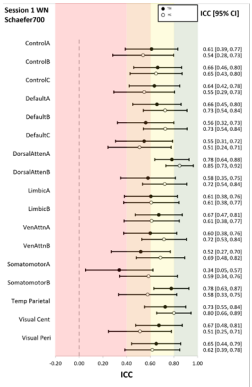

Note. Values are ICCs along with 95% confidence interval in brackets. ICCs are provided for each of the 17 networks in the Schaefer 700 atlas. WN = within-network connectivity.

Figure 29

ICCs Session 2: Schaefer 700 WN Reliability

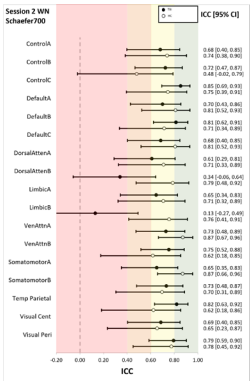

Note. Values are ICCs along with 95% confidence interval in brackets. ICCs are provided for each of the 17 networks in the Schaefer 700 atlas. WN = within-network connectivity.

Figure 30

ICCs Session 1: Schaefer 700 Segregation Reliability

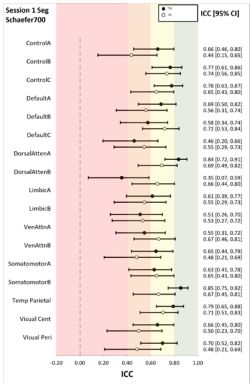

Note. Values are ICCs along with 95% confidence interval in brackets. ICCs are provided for each of the 17 networks in the Schaefer 700 atlas. Seg = segregation.

Figure 31

ICCs Session 2: Schaefer 700 Segregation Reliability

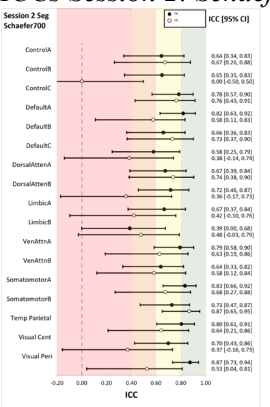

Note. Values are ICCs along with 95% confidence interval in brackets. ICCs are provided for each of the 17 networks in the Schaefer 700 atlas. Seg = segregation.

Figure 32

ICCs Session 1: Schaefer 1000 WN Reliability

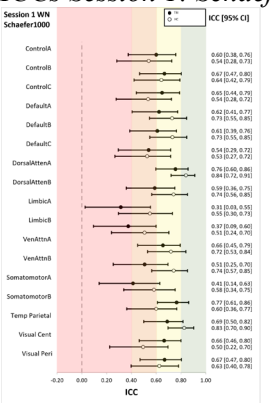

Note. Values are ICCs along with 95% confidence interval in brackets. ICCs are provided for each of the 17 networks in the Schaefer 1000 atlas. WN = within-network connectivity.

Figure 33

ICCs Session 2: Schaefer 1000 WN Reliability

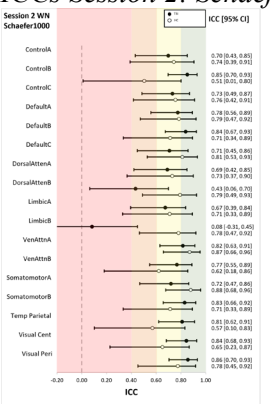

Note. Values are ICCs along with 95% confidence interval in brackets. ICCs are provided for each of the 17 networks in the Schaefer 1000 atlas. WN = within-network connectivity.

Figure 34

ICCs Session 1: Schaefer 1000 Segregation Reliability

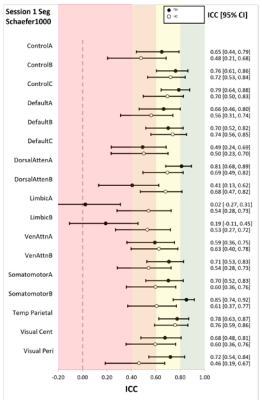

Note. Values are ICCs along with 95% confidence interval in brackets. ICCs are provided for each of the 17 networks in the Schaefer 1000 atlas. Seg = segregation.

Figure 35

ICCs Session 2: Schaefer 1000 Segregation Reliability

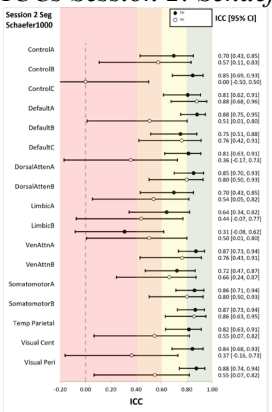

Note. Values are ICCs along with 95% confidence interval in brackets. ICCs are provided for each of the 17 networks in the Schaefer 1000 atlas. Seg = segregation.

Appendix B

Tables

Table 1
Session 1: Demographic Information

	TBI group (*N*=45)		HC group (*N*=41)	
Characteristic	*M*	*SD*	*M*	*SD*
Age	63.40	7.88	65.02	7.10
Education (Years)	14.04	2.88	16.37	2.40
Time Post Injury (Years)	9.02	5.42	–	–
PTA (Days)	22.86	27.91	–	–
GCS	11.45	4.11	–	–
% Complicated mild	29% (*N*=13)		–	
% Moderate	27% (*N*=12)		–	
% Severe	44% (*N*=20)		–	
Sex	32 Male, 13 Female		24 Male, 17 Female	
Ethnicity	1 Hispanic		0 Hispanic	
Race	34 White/Caucasian, 11 Black/African-American		32 White/Caucasian, 9 Black/African-American	

Table 2
Session 2: Demographic Information

	TBI group (*N*=25)		HC group (*N*=15)	
Characteristic	*M*	*SD*	*M*	*SD*
Age	65.28	8.17	65.33	6.56
Education (Years)	14.32	2.98	15.93	2.82
Time Post Injury (Years)	11.97	5.26	–	–
PTA (Days)	30.35	31.17	–	–
GCS	10.20	4.56	–	–
% Complicated mild	16% (*N*=4)		–	
% Moderate	20% (*N*=5)		–	
% Severe	64% (*N*=16)		–	
Sex	16 Male, 9 Female		7 Male, 8 Female	
Ethnicity	1 Hispanic		0 Hispanic	
Race	17 White/Caucasian, 8 Black/African-American		11 White/Caucasian, 4 Black/African-American	

Table 3

Schaefer Network Reliability for WN Connectivity

	Average WN ICC Reliability for Schaefer Atlases							
Network	Session 1				Session 2			
	S100	S400	S700	S1000	S100	S400	S700	S1000
ControlA								
TBI	F	F	G	G	G	G	G	G
HC	F	G	F	F	G	G	G	G
ControlB								
TBI	G	F	G	G	G	G	G	E
HC	F	G	G	G	P	G	F	F
ControlC								
TBI	F	G	G	G	G	G	E	G
HC	F	G	F	F	G	E	G	G
DefaultA								
TBI	G	G	G	G	G	G	G	G
HC	G	G	G	G	E	G	E	G
DefaultB								
TBI	F	G	F	G	G	G	E	E
HC	G	E	G	G	G	F	G	G
DefaultC								
TBI	F	F	F	F	F	G	G	G
HC	F	F	F	F	F	G	E	E
DorsalAttenA								
TBI	G	F	G	G	G	G	G	G
HC	G	G	E	E	F	G	G	G
DorsalAttenB								
TBI	F	F	F	F	F	G	P	F
HC	F	F	G	G	E	G	G	G
LimbicA								
TBI	E	F	G	P	E	G	G	G
HC	G	F	G	F	F	G	G	G
LimbicB								
TBI	F	E	G	P	F	F	P	P
HC	F	G	G	F	F	F	G	G
Salience/VenAttnA								
TBI	F	G	G	G	G	F	G	E
HC	F	E	G	G	G	G	E	E
Salience/VenAttnB								
TBI	F	F	F	F	G	P	G	G
HC	G	G	G	G	G	G	G	G
SomatomotorA								
TBI	P	G	P	F	F	E	G	G
HC	F	F	F	F	E	G	E	E
SomatomotorB								
TBI	G	G	G	G	G	G	G	E
HC	F	G	F	G	G	E	G	G
TemporalParietal								

TBI	F	G	G	G	F	E	E	E
HC	G	F	E	E	F	E	G	F
VisualCent								
TBI	F	F	G	G	P	G	G	E
HC	F	F	F	F	F	G	G	G
VisualPeri								
TBI	G	G	G	G	G	G	G	E
HC	F	F	G	G	F	P	G	G

Note. ICCs are color-coded using reliability criteria from Ma et al. (2021). This table combines data from all Schaefer atlases. E = excellent; G = good; F = fair; P = poor; S100 = Schaefer100; S400 = Schaefer400; S700 = Schaefer700; S1000 = Schaefer1000.

Table 4

Schaefer Network Reliability for Segregation

	Average Segregation Reliability for Schaefer Atlases							
Network	Session 1				Session 2			
	S100	S400	S700	S1000	S100	S400	S700	S1000
ControlA								
TBI	F	F	G	G	G	G	G	G
HC	P	F	F	F	E	G	G	F
ControlB								
TBI	G	F	G	G	G	G	G	E
HC	F	F	G	G	P	G	P	P
ControlC								
TBI	G	G	G	G	G	E	G	E
HC	F	F	G	G	F	G	G	E
DefaultA								
TBI	F	E	G	G	G	G	E	E
HC	F	G	F	F	P	E	F	F
DefaultB								
TBI	F	G	F	G	G	G	G	G
HC	G	G	G	G	G	G	G	G
DefaultC								
TBI	G	F	F	F	F	G	F	E
HC	F	F	F	F	F	F	P	P
DorsalAttnA								
TBI	G	F	E	E	G	G	G	E
HC	G	G	G	G	G	F	G	G
DorsalAttnB								
TBI	P	F	P	F	G	G	G	G
HC	G	F	G	G	G	F	P	F
LimbicA								
TBI	G	P	G	P	P	F	G	G
HC	G	P	F	F	G	P	F	F
LimbicB								
TBI	P	P	F	P	G	P	P	P
HC	P	F	F	F	P	G	F	F
Salience/VenAttnA								

TBI	G	G	F	F	G	G	G	E
HC	G	G	G	G	F	G	G	G
Salience/VenAttnB								
TBI	E	P	G	G	F	G	G	G
HC	F	G	F	F	G	F	F	G
SomatomotorA								
TBI	F	G	G	G	G	G	E	E
HC	F	G	G	F	G	G	G	E
SomatomotorB								
TBI	F	G	E	E	G	E	G	E
HC	F	F	G	G	F	G	E	E
TemporalParietal								
TBI	F	G	G	G	P	G	E	E
HC	F	F	G	G	G	G	G	F
VisualCent								
TBI	F	G	G	G	P	F	G	E
HC	G	F	F	F	F	G	F	P
VisualPeri								
TBI	P	G	G	G	G	F	E	E
HC	P	G	F	F	E	G	F	F

Note. ICCs are color-coded using reliability criteria from Ma et al. (2021). This table combines data from all Schaefer atlases. E = excellent; G = good; F = fair; P = poor; S100 = Schaefer100; S400 = Schaefer400; S700 = Schaefer700; S1000 = Schaefer1000.

Table 5

Power Network Reliability for WN Connectivity and Segregation

	Average WN Connectivity and Segregation Reliability for Power Atlas			
Network	WN		Segregation	
	Session 1	Session 2	Session 1	Session 2
SensoryHand				
TBI	G	G	G	G
HC	F	E	G	G
SensoryMouth				
TBI	F	G	F	G
HC	G	E	F	F
CinguloTaskControl				
TBI	G	G	G	G
HC	G	G	F	F
Auditory				
TBI	F	P	F	G
HC	G	E	P	F
Default				
TBI	G	G	E	G
HC	G	G	G	E
Visual				
TBI	F	G	G	F

HC	F	G	F	P
FrontoparietalTask				
TBI	G	G	G	E
HC	G	E	G	G
Salience				
TBI	F	G	F	G
HC	G	E	F	P
Subcortical				
TBI	F	P	P	F
HC	G	E	G	G
VentralAttn				
TBI	F	F	F	F
HC	F	F	F	P
DorsalAttn				
TBI	F	G	F	P
HC	G	E	F	F
Cerebellar				
TBI	G	F	G	G
HC	F	E	G	G

Note. ICCs are color-coded using reliability criteria from Ma et al. (2021). This table combines data from all Schaefer atlases. E = excellent; G = good; F = fair; P = poor.

Table 6

Brainnetome Network Reliability for WN Connectivity and Segregation

	Average WN Connectivity and Segregation Reliability for Brainnetome Atlas			
Network	WN		Segregation	
	Session 1	Session 2	Session 1	Session 2
Visual1				
TBI	G	G	G	G
HC	F	G	F	G
Visual2				
TBI	G	G	G	G
HC	F	F	G	P
Sensorimotor1				
TBI	G	G	F	G
HC	F	G	F	F
Sensorimotor2				
TBI	G	G	F	G
HC	G	E	F	G
DorsalAttn1				
TBI	F	G	F	G
HC	G	G	G	G
DorsalAttn2				
TBI	F	G	F	F
HC	P	G	F	G
VentralAttn				
TBI	G	F	G	G

HC	G	G	G	G
Frontoparietal1				
TBI	F	P	F	F
HC	G	G	F	F
Limbic1				
TBI	F	G	F	G
HC	G	E	G	G
Limbic2				
TBI	G	G	G	P
HC	F	F	F	F
Frontoparietal2				
TBI	F	G	P	G
HC	F	F	F	F
Frontoparietal3				
TBI	F	G	F	G
HC	F	G	P	P
Frontoparietal4				
TBI	F	G	P	F
HC	F	G	F	P
Sensorimotor3				
TBI	G	G	G	G
HC	F	E	F	G
Default1				
TBI	F	G	F	F
HC	F	G	P	F
Default2				
TBI	G	G	G	G
HC	G	G	G	E
Default3				
TBI	F	G	F	G
HC	G	G	F	G
Subcortical				
TBI	F	F	F	G
HC	E	E	E	G
Cerebellar				
TBI	G	G	G	E
HC	G	E	G	E

Note. ICCs are color-coded using reliability criteria from Ma et al. (2021). This table combines data from all Schaefer atlases. E = excellent; G = good; F = fair; P = poor.

Table 7

Gordon Network Reliability for WN Connectivity and Segregation

	Average WN Connectivity and Segregation Reliability for Gordon Atlas			
Network	WN		Segregation	
	Session 1	Session 2	Session 1	Session 2
Default				
TBI	G	G	G	G

HC	G	E	E	G
SmHand				
TBI	F	G	G	F
HC	G	F	F	G
SmMouth				
TBI	G	G	G	F
HC	F	G	G	G
Visual				
TBI	F	G	G	G
HC	G	E	G	G
Frontoparietal				
TBI	F	G	G	F
HC	F	F	F	P
Auditory				
TBI	F	G	G	G
HC	G	G	G	G
CinguloParietal				
TBI	G	G	G	F
HC	G	G	F	F
RetrosplenialTemp				
TBI	G	G	G	G
HC	G	E	G	E
CinguloOperc				
TBI	G	F	G	G
HC	F	P	F	P
Ventral Attn				
TBI	G	F	E	E
HC	G	G	F	G
Salience				
TBI	G	G	G	G
HC	G	G	F	P
DorsalAttn				
TBI	F	G	P	F
HC	F	P	P	P

Note. ICCs are color-coded using reliability criteria from Ma et al. (2021). This table combines data from all Schaefer atlases. E = excellent; G = good; F = fair; P = poor.

Table 8

Glasser Network Reliability for WN Connectivity and Segregation

	Average WN Connectivity and Segregation Reliability for Glasser Atlas			
Network	WN		Segregation	
	Session 1	Session 2	Session 1	Session 2
Visual1				
TBI	P	P	P	G
HC	F	G	F	P
Visual2				
TBI	F	G	F	F

HC	F	E	P	P
Somatomotor				
TBI	F	G	F	G
HC	G	G	F	P
CinguloOperc				
TBI	F	G	F	F
HC	G	G	F	P
Language				
TBI	F	G	P	G
HC	G	G	P	F
Default				
TBI	G	G	F	F
HC	F	G	P	P
Frontoparietal				
TBI	G	F	F	G
HC	F	G	F	P
Auditory				
TBI	F	G	P	G
HC	P	G	P	F
Post-Multi				
TBI	G	G	G	F
HC	F	G	P	F
DorsalAttn				
TBI	P	G	F	F
HC	F	G	P	P
VentralMult				
TBI	G	F	P	P
HC	F	P	P	P
OrbitoAffect				
TBI	P	F	F	F
HC	P	P	P	P

Note. ICCs are color-coded using reliability criteria from Ma et al. (2021). This table combines data from all Schaefer atlases. E = excellent; G = good; F = fair; P = poor.